ARTICLE

Model dialkyl peroxides of the Fenton mechanistic probe 2-methyl-1-phenyl-2-propyl hydroperoxide (MPPH): kinetic probes for dissociative electron transfer

David C. Magri and Mark S. Workentin *

Department of Chemistry, The University of Western Ontario, London, ON, Canada N6A 5B7

Two dialkyl peroxides, devised as kinetic probes for the heterogeneous electron transfer (ET), are studied using heterogeneous and homogeneous electrochemical techniques. The peroxides react by concerted dissociative ET reduction of the O–O bond. Under heterogeneous conditions, the only products isolated are the corresponding alcohols from a two-electron reduction as has been observed with other dialkyl peroxides studied to date. However, under homogeneous conditions, a generated alkoxyl radical undergoes a rapid β-scission fragmentation in competition with the second ET resulting in formation of acetone and a benzyl radical. With knowledge of the rate constant for fragmentation and accounting for the diffuse double layer at the electrode interface, the heterogeneous ET rate constant to the alkoxyl radicals is estimated to be 1500 cm s^{-1}. The heterogeneous and homogeneous ET kinetics of the O–O bond cleavage have also been measured and examined as a function of the driving force for ET, ΔG_{ET}, using dissociative electron transfer theory. From both sets of kinetics, besides the evaluation of thermochemical parameters, it is demonstrated that the heterogeneous and homogeneous reduction of the O–O bond appears to be non-adiabatic.
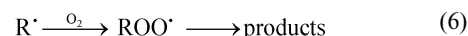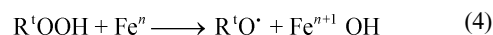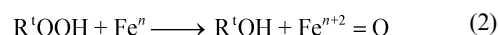
Introduction

In recent years, there have been many claims of successfully mimicking the elegant chemistry of monooxygenases, enzymes that use molecular oxygen to selectively functionalise saturated hydrocarbons (eqn. (1)).[1–9] Many of these ubiquitous enzymes such as the cytochrome P450s,[10–12] peroxidases,[13] and catalases[13] contain an iron(III) protoporphyrin IX complex, whereas methane monooxygenases,[14,15] found only in methanotrophic bacteria, contain a (μ-oxo) di-iron complex. Substantial evidence suggests the active intermediate in the oxidative mechanism of heme enzymes is an oxo-iron(IV) porphyrin π-radical cation [PFe^{IV}=O]$^{•+}$.[11,16,17]

$$RH + O_2 \xrightarrow[+\,2\,H^+ +\,2e^-]{\text{enzyme}} ROH + H_2O \qquad (1)$$

In attempts to mimic the aforementioned enzymes, most biomimetic systems have utilised an Fe(II) or Fe(III) complex as the catalyst and H$_2$O$_2$ or a tertiary hydroperoxide (R^{t}OOH), such as *tert*-butyl hydroperoxide (TBHP), as the oxidant. A notable example is work by Que and colleagues who have characterised and studied both mono-iron(III) and (μ-oxo) di-iron(III) complexes containing tetradentate, tripodal tris-(pyridylmethyl)amine (TPA) ligands.[4–8,18–20] The oxidation of various saturated hydrocarbons in the presence of these iron catalysts has been achieved and found to yield not only alcohols (eqn. (1)) but other products such as ketones and dialkyl peroxides. It was initially proposed that the mechanism of action involved heterolysis of the hydroperoxide O–O bond generating a high-valent iron-oxo species,[5,6] Fe^{IV}=O or Fe^V=O (eqn. (2)), analogous to that observed with the monooxygenase enzymes,[10] the exact high-valent iron-oxo species dependent on the initial oxidation state of the metal catalyst. Subsequently, the high-valent iron-oxo species was presumed to abstract a hydrogen atom from the hydrocarbon, and "insert" an oxygen atom into the substrate regenerating the catalyst (eqn. (3)).[5,6] Indirect evidence for the existence of a nonheme Fe^{IV}=O intermediate has been invoked based on mechanistic studies,[21–23] but most recently supported by a crystallographic and spectroscopic study.[24] On the contrary, evidence for a nonheme Fe^V=O intermediate is supported solely on mechanistic studies.[7,8,25]

An alternative mechanism has been postulated to rationalise the chemistry observed with the nonheme biomimetic catalysts. Substantial evidence supports alkoxyl radicals as the reactive intermediate and not high-valent iron-oxo species.[26–34] The initial step of this proposed mechanism involves homolysis of the O–O bond by electron transfer (ET) from the iron catalyst to the hydroperoxide (eqn. (4)).[30,34–36] The generated alkoxyl radical then abstracts a hydrogen atom from the saturated hydrocarbon to afford a carbon radical (eqn. (5)). Under aerobic conditions, the carbon radical reacts with dioxygen forming a peroxyl radical leading to alkane oxidation products (eqn. (6)).[26–30,36] In both of these mechanistic possibilities, the catalyst, represented as Fe^n, can have either the Fe^{II} or Fe^{III} oxidation state.

$$R^tOOH + Fe^n \longrightarrow R^tOH + Fe^{n+2} = O \qquad (2)$$

$$Fe^{n+2} = O + RH \longrightarrow Fe^n + ROH \qquad (3)$$

$$R^tOOH + Fe^n \longrightarrow R^tO^{\bullet} + Fe^{n+1}\,OH \qquad (4)$$

$$R^tO^{\bullet} + RH \longrightarrow R^tOH + R^{\bullet} \qquad (5)$$

$$R^{\bullet} \xrightarrow{O_2} ROO^{\bullet} \longrightarrow \text{products} \qquad (6)$$

To differentiate biomimetic oxidations from oxidations mediated by freely diffusing radicals[36]—heterolytic (eqn. (2)) *versus* homolytic (eqn. (4)) O–O bond cleavage—Ingold, Wayner, and co-workers devised the mechanistic probe 2-methyl-1-phenyl-2-propyl hydroperoxide (MPPH).[26] The characteristic feature of the MPPH probe is the rapid β-scission fragmentation ($k_{\beta} \sim 2.2 \times 10^8$ s^{-1}) of the corresponding alkoxyl radical (eqn. (7)).[26] The MPPH alkoxyl radical has a short lifetime (5 ns), much shorter than the *tert*-butoxyl radical, and too short to abstract a hydrogen atom from a saturated hydrocarbon. With MPPH, hydrogen abstraction of the alkane by the MPPH alkoxyl radical does not occur (eqn. (5)) and instead the radical fragments to acetone and a benzyl radical (eqn. (7)), which is the only species subsequently oxidised. In the presence of air, the benzyl radical reacts with dioxygen forming a
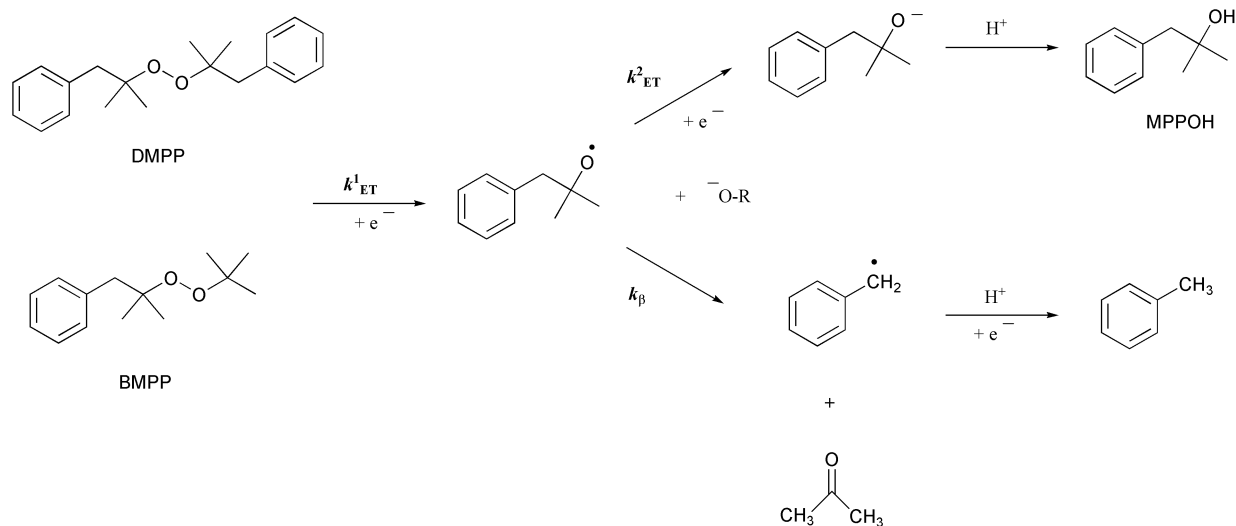
Scheme 1 The competitive reaction pathways, reduction and β-scission fragmentation, available to the MPPH alkoxyl radical after dissociative electron transfer to the dialkyl peroxides DMPP and BMPP. The rate constants k^1_{ET} and k^2_{ET} are used generically to represent either a heterogeneous or homogeneous ET. In the text, a distinction is made by replacing the subscript ET with the subscript het or hom.

benzylperoxyl radical yielding a large quantity of benzaldehyde, whereas under an inert atmosphere, benzyl alcohol is the major product.[21,22,28,29]

$$PhCH_2CMe_2O^\bullet \xrightarrow{k_\beta} PhCH_2^\bullet + Me_2CO \qquad (7)$$

Despite the wealth of information known about the chemistry of the MPPH alkoxyl radical and the follow-up chemistry (eqn. (7)), little is known about the initial ET to the O–O bond of MPPH (eqn. (4)). The usefulness of MPPH as a mechanistic probe, in general, would be greatly enhanced if the rates of ET from potential donors were known. Furthermore, knowledge of the standard reduction potential of MPPH would allow the feasibility for ET from potential donors to be predicted. By applying theories of ET, the driving force of the reaction can be related to the kinetics, and from such an analysis, other inherent properties of MPPH can be determined.

One way of determining thermodynamic and kinetic information about a substrate, such as standard reduction potentials and kinetic rate constants, is by using various electrochemical techniques. Unfortunately, hydroperoxides are prone to rapid decomposition under reductive electrochemical conditions because of the acidic peroxy proton, thus preventing such information from being easily determined. On the other hand, dialkyl peroxides lacking α-protons adjacent to the O–O bond are robust to base-induced decomposition. Keeping these structural considerations in mind, we devised two dialkyl peroxides as models for MPPH (see Scheme 1) in order to gain some insight into its ET chemistry and intrinsic properties.

The study of the ET reduction of peroxides and endoperoxides is an active area of research by our group[37–42] and the group of Maran and co-workers.[43–48] Besides playing important roles in a number of biological and chemical processes,[49–51] peroxides and endoperoxides also provide intriguing model systems for testing Savéant's dissociative electron transfer (DET) theory.[52–54] In general, DET systems are characterised by the concerted cleavage of a σ bond upon ET, resulting in the formation of reactive species such as radicals and ions. In most case studies, ET to O–O bonds has been observed to be a concerted dissociative process,[37–44] although examples of a stepwise dissociative mechanism[44–48] have also been observed. Substantial evidence has also revealed that ET to O–O bonds is non-adiabatic.[37,38,44] This behaviour is manifested in ET rate constants smaller than predicted by adiabatic ET models.

Regardless of the mechanistic route, concerted or stepwise, upon O–O bond fragmentation the products from the ET to dialkyl peroxides are an alkoxyl radical and an alkoxide (eqn. (8)). Under heterogeneous conditions, the alkoxyl radical is generated at the electrode surface at a potential much more negative than its reduction potential. Because of the favourable driving force for ET, generally in excess of −1.0 V, the alkoxyl radical is reduced at the electrode interface before escaping into the bulk solution. In only two examples has some other alkoxyl reactivity been observed in competition with the second heterogeneous ET (eqn. (9)).[39,40] Intuitively, based on the large driving force for ET, it is assumed the rate of the heterogeneous ET to the alkoxyl radical is extremely fast, faster than the rate of diffusion away from the electrode surface; however, up to now no attempt has been made to quantify the rate constant of this process (eqn. (9)).

$$ROOR \xrightarrow{+e^-} RO^\bullet + {}^-OR \qquad (8)$$

$$RO^\bullet + {}^-OR \xrightarrow{+e^-} 2RO^- \qquad (9)$$
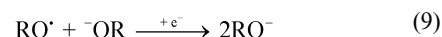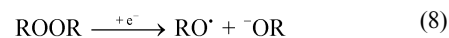
In this article, the dialkyl peroxides di-2-methyl-1-phenyl-2-propyl peroxide (DMPP) and *tert*-butyl 2-methyl-1-phenyl-2-propyl peroxide (BMPP) are studied using heterogeneous and homogeneous electrochemical techniques in aprotic solvents. These two peroxides were devised as kinetic probes for the heterogeneous ET rate constant to alkoxyl radicals initiated by dissociative electron transfer (eqn. (9)). Product studies were conducted to investigate the partitioning ratio between the reaction pathways available to the MPPH alkoxyl radical, reduction and β-scission fragmentation, and from knowledge of the rate constant of β-scission ($k_\beta \sim 2.2 \times 10^8$ s^{-1}) we have quantified the rate constant of the second heterogeneous ET (k^2_{het}) to the MPPH alkoxyl radical (eqn. (9)). In addition, the heterogeneous (k^1_{het}) and homogeneous (k^1_{hom}) ET kinetics of DMPP and BMPP have been measured in *N,N*-dimethylformamide. Cyclic voltammetry in conjunction with a thermochemical cycle is used to evaluate the dissociative standard reduction potential (E°_{diss}) of each peroxide and used to relate the kinetics to the driving force for ET, ΔG_{ET}. We also provide further evidence that ET to the O–O bond is non-adiabatic,[37,38,44] and accounting for this behaviour, evaluate a number of thermochemical parameters for these two model compounds. The knowledge gained from the study of these dialkyl peroxides has relevance not only to the dissociative chemistry of peroxides in general, but also to the employment of MPPH as a mechanistic probe in biomimetic systems.

Table 1 Cyclic voltammetry data for the cathodic reduction of DMPP and BMPP in N,N-dimethylformamide (DMF) and acetonitrile (ACN) in the presence of 0.10 M TEAP at 25 °C measured at a glassy carbon electrode

	Scan rate/V s^{-1}	DMPP[a] DMF	DMPP[a] ACN	BMPP[a] DMF	BMPP[a] ACN
E_p/V $vs.$ SCE[b]	0.1	−2.16	−2.12	−2.34	−2.30
	1.0	−2.27	−2.23	−2.46	−2.42
	10	−2.40	−2.37	−2.60	−2.60
$E_{p/2} - E_p$/V $vs.$ SCE[b]	0.1	0.188	0.192	0.188	0.194
	1.0	0.200	0.211	0.203	0.221
	10	0.259	0.248	0.280	0.260
$a = 1.857RT/F(E_{p/2} - E_p)$	0.1	0.254	0.249	0.254	0.246
	1.0	0.239	0.226	0.235	0.221
	10	0.184	0.192	0.170	0.184
$a = 1.15RT/F(dE_p/d(\log v))$		0.23	0.23	0.22	0.22
$-(dE_p/d(\log v))$/mV		127	129	134	133
n (# of electrons)		2.0[c]	2.1	2.0	2.0

[a] Potentials are referenced $versus$ ferrocene: 0.449 V and 0.475 V $vs.$ SCE in ACN and DMF. [b] $dE_p/d(\log v)$ based on scan rates between 0.1 and 10 V s^{-1}. [c] In presence of non-nucleophilic acids: $n = 1.9$ (2,2,2-trifluoroethanol), $n = 2.2$ (acetanilide).

Results

Cyclic voltammetry

The reduction of DMPP and BMPP was studied in solutions of N,N-dimethylformamide (DMF) and acetonitrile (ACN) containing 0.10 M tetraethylammonium perchlorate (TEAP) using a glassy carbon working electrode at 25 °C. Cyclic voltammetry of both peroxides is characterised by a broad and chemically irreversible cathodic peak at all scan rates investigated between 0.1 and 50 V s^{-1}. The peak potentials, E_p, at 0.1 V s^{-1} $vs.$ SCE are −2.16 and −2.34 V in DMF and −2.12 and −2.30 V in ACN, respectively, for DMPP and BMPP. Increasing the scan rate, v, shifts the E_p linearly to more negative potentials from −127 to −134 mV (log v)$^{-1}$ and broadens the cathodic wave (peak width: $\Delta E_{p/2} = E_{p/2} - E_p$) from 188 mV at 0.1 V s^{-1} to 280 mV at 10 V s^{-1}. The $\Delta E_{p/2}$, and peak height, I_p, of the voltammograms are unaffected by the addition of weak non-nucleophilic acids such as 2,2,2-trifluoroethanol and acetanilide. A summary of the voltammetry data in both solvents is reported in Table 1.

An irreversible anodic peak, generated after the initial reduction, is observed in both solvents at roughly −0.2 V $vs.$ SCE at 0.1 V s^{-1}. It is attributed to the oxidation of alkoxides formed from the initial reduction of the peroxide, as independently confirmed for DMPP by an authentic sample of MPPOH in the presence of tetraethylammonium hydroxide. In ACN, a second anodic peak is observed at slightly more negative potentials on increasing the scan rate and attributed to some other electrochemically generated base. These anodic peaks (only the more positive peak in ACN was examined) were found to increase with scan rate and to experimentally shift in the positive direction by 31.5 mV (log v)$^{-1}$ in accordance with a first order irreversible process.[55,56] Cyclic voltammographs of DMPP and BMPP in the absence and presence of the 2,2,2-trifluoroethanol are shown in Fig. 1.

The transfer coefficient, a, is a diagnostic parameter, which reflects how the free energy of activation, $\Delta G^{\neq}$, varies with the driving force for ET, ΔG_{ET}. It can be used as an indication of whether ET occurs by a stepwise ($a \cong 0.5$) or a concerted mechanism ($a << 0.5$).[52,53] In our analysis, a was determined two ways: i) from the scan rate dependence of the irreversible peak $a = 1.15RT/[dE_p/(d\log v)]$ and ii) from the corresponding peak width at each scan rate $a = 1.857RT/(F\Delta E_{p/2})$.[56] The first approach yields average values of 0.23 and 0.22 for DMPP and BMPP; the second approach gives a decreasing range of a values from 0.25 at 0.1 V s^{-1} to 0.17 at 10 V s^{-1}. A summary of the a values is included in Table 1. Such low a values are an indication that ET to DMPP and BMPP occurs by a concerted dissociative mechanism.[52,53] Furthermore, the scan rate dependence of the E_p, and the fact that the normalised peak
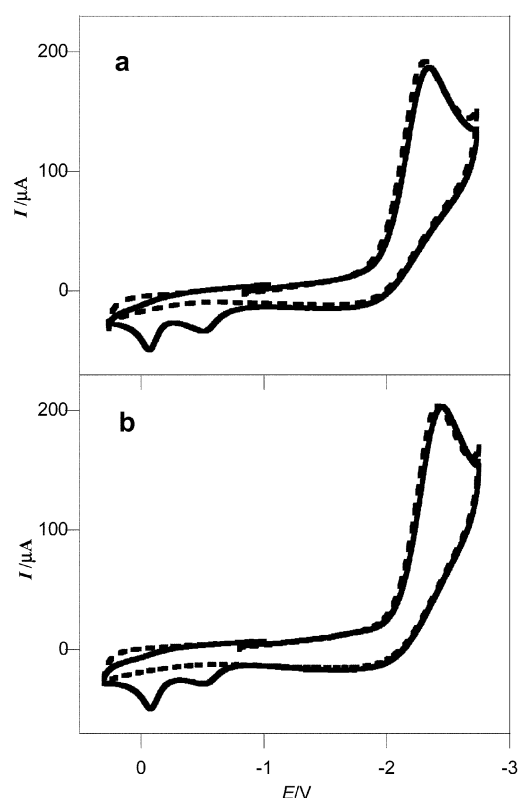

Fig. 1 Cyclic voltammograms of 2.0 mM (a) DMPP at 1.0 V s^{-1} and (b) BMPP at 0.8 V s^{-1} in 0.10 M TEAP–acetonitrile solution in the absence (—) and presence (----) of 5 mM 2,2,2-trifluoroethanol.

current, $i_p/v^{1/2}$, decreases with scan rate indicates the initial ET is the rate-determining step and cannot be described using Butler–Volmer kinetics.[57] As a consequence, the standard reduction potential ($E°_{diss}$) and standard heterogeneous rate constant ($k°_{het}$) cannot be determined directly from the cyclic voltammetry ($vide\ infra$).

Heterogeneous product studies

Constant potential electrolyses of both peroxides were carried out with a glassy carbon rotating disk electrode (or a platinum foil). The experimentally determined coulometry values are included in Table 1. In all cases, 2 F mol^{-1} of charge is consumed independent of solvent, electrode material and the presence of weak acid. Work-up of the electrolysed solution of DMPP and quantification by GC yielded only 2-methyl-1-phenyl-2-propanol (MPPOH) in an average isolated yield of 65%. In the case of BMPP, the recovered yield of MPPOH was

Table 2 Data acquired from the convolution analysis of DMPP and BMPP in *N*,*N*-dimethylformamide (DMF) and acetonitrile (ACN) in the presence of 0.10 M TEAP at 25 °C at a glassy carbon electrode
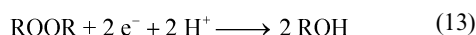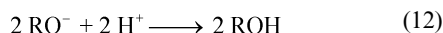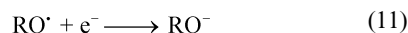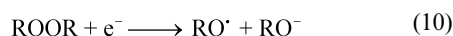
	DMPP DMF	DMPP ACN	BMPP DMF	BMPP ACN
D^{ab}/cm^2 s^{-1}	4.87×10^{-6}	1.16×10^{-5}	6.68×10^{-6}	1.47×10^{-5}
$E^{\circ}_{diss}{}^c$/V	-1.20	-1.22	-1.26	-1.30
log ($k^{\circ}_{het}{}^d$/cm s^{-1})	-6.7	-6.5	-6.8	-6.3
$\Delta G_0^{\neq e}$/kcal mol^{-1}	10.8	12.4	11.8	10.5

[a] These values are validated by the diffusion coefficient ratios (ACN/DMF), which are 2.38 and 2.20 for DMPP and BMPP in excellent agreement with the ratio between the viscosity of the solvents: 0.796/0.344 = 2.31. [b] Ferrocene diffusion coefficients of 1.13×10^{-5} and 2.38×10^{-5} cm^2 s^{-1} in DMF and ACN were used to calculate the area of the electrode from reference 38*a*. [c] Estimated error is ± 0.20 V and uncorrected for the double layer. [d] Estimated error ± 0.8 approximated by digital simulation of experimental CVs from 0.1 to 10 V s^{-1} using the *a* values reported in Table 1 and the experimental E°_{diss} values. [e] $\Delta G_0^{\neq}$ determined from the slope of *a vs. E* plots and $\Delta G_0^{\neq} = F/[8(da/dE)]$.

similar. *tert*-Butanol, on the other hand, was not quantified due to its high solubility in water and volatility, although it was detected by ^{1}H NMR spectroscopy as a singlet at 1.26 ppm.

Fragmentation products such as toluene or acetone were not detected upon work-up suggesting under heterogeneous conditions that β-scission fragmentation of the alkoxyl radicals does not compete, at least to a measurable extent, with the second heterogeneous ET. Admittedly, the isolated yields of MPPOH are not quantitative. Further support for the lack of fragmentation products was obtained by digital simulation of the experimental voltammograms using the determined parameters from Tables 1 and 2 and by monitoring the concentration profiles at several hundreds millivolts past the peak potential. Simulations with k_β equal to 2.2×10^8 s^{-1} predicted the formation of alcohols in greater than 99% yield. An increase in k_β by one and two orders of magnitude, respectively, would yield approximately 2% and 6% fragmentation products. Thus, the coulometry, product analysis, and voltammetry are consistent with the steps outlined in eqns. (10)–(12), with an overall two-electron dissociative ET mechanism[38,43,44] described by eqn. (13).

$$\text{ROOR} + \text{e}^- \longrightarrow \text{RO}^{\bullet} + \text{RO}^- \qquad (10)$$

$$\text{RO}^{\bullet} + \text{e}^- \longrightarrow \text{RO}^- \qquad (11)$$

$$2\,\text{RO}^- + 2\,\text{H}^+ \longrightarrow 2\,\text{ROH} \qquad (12)$$

$$\text{ROOR} + 2\,\text{e}^- + 2\,\text{H}^+ \longrightarrow 2\,\text{ROH} \qquad (13)$$

Heterogeneous kinetics

Convolution analysis was used to evaluate the kinetics (k^1_{het}) of the heterogeneous reduction of BMPP and DMPP at a glassy carbon electrode in both DMF and ACN. The method has been successfully applied to a number of peroxide systems.[37,38,41,43–48] The experimental and theoretical details of the technique are described in detail elsewhere.[58–60] Briefly, a series of high-quality cyclic voltammograms were obtained between the scan rates of 0.1 and 10 V s^{-1} at 1 or 2 points per mV data acquisition and the corresponding backgrounds subtracted. The normalised cyclic voltammograms (*i–E* curves) were then transformed into sigmoidal-shaped curves by use of the convolution integral.[61] The maximum limiting currents, I_{lim}, of the transformed curves were in excellent agreement with a margin of error less than 3%. From the determined I_{lim} and the known area of the glassy carbon electrode (determined separately by analysis of ferrocene with literature diffusion coefficients), the diffusion coefficients, D, of BMPP and DMPP in the presence of 0.10 M TEAP in DMF and ACN were determined. From the *i* and I_{lim} values, the potential dependence of both k^1_{het} and *a* is evaluated.[62] E°_{diss} were estimated from extrapolation of *a–E* plots corresponding to *a* = 0.5. By this method, approximate values of E°_{diss} between -1.2 and -1.3 V were obtained in both

solvents. The k°_{het} was estimated from the second order fit to the heterogeneous kinetics at E°_{diss}. The k°_{het} are low with average values of 2.0×10^{-7} and 4.0×10^{-7} cm s^{-1} in DMF and ACN, which results in the peak potential being more negative than the estimated E°_{diss} by 0.8 V. A complete summary of the extracted parameters D, k°_{het}, E°_{diss} and intrinsic barrier, $\Delta G_0^{\neq}$, is included in Table 2. These values are consistent with those determined for other dialkyl peroxides.[38,43] The experimental values were finally checked by digital simulation of the cyclic voltammograms including the second heterogeneous ET rate constant (k^2_{het}) determined in this study (*vide infra*) resulting in good agreement between the experimental and simulated results.

Homogeneous product studies

The indirect electrolysis of DMPP and BMPP was studied using electrochemically generated outer-sphere ET radical anion donors to determine if the β-scission fragmentation can compete with the second ET under homogeneous conditions. Mediators were carefully selected to eliminate the possibility of nucleophilic addition of the benzyl anion[63] and studies were performed in ACN because of a known complicating side reaction in DMF.[64] The results from the homogeneous product studies of DMPP and BMPP are reported in Tables 3 and 4. The data are reported as mole % based on the consumption of peroxide. In all studies with DMPP no starting peroxide was recovered. However, with BMPP and mediators at less negative reduction potentials ($E^{\circ} > -1.5$ V), which are not catalytic because of the slower reaction rates, some unreacted peroxide was recovered. Also reported in the tables are the standard reduction potential of the donors in ACN and the electron equivalents consumed in the indirect electrolysis. For all the products the maximum possible yield is 100%, with the exception of MPPOH from DMPP, in which case the maximum possible yield is 200%.

As can be seen in Tables 3 and 4, the indirect electrolysis is a two-electron (*n* = 2) process. With donors of more negative reduction potentials ($E^{\circ} < -1.7$ V), the donor recovery was always > 98%, with the exception of anthracene where a small amount of dihydroanthracene was recovered. The major quantifiable products from both peroxides are MPPOH and toluene, with bibenzyl as a minor product detected in trace amounts.[65] Formation of toluene and bibenzyl is conclusive evidence β-scission fragmentation of the MPPH alkoxyl radical, generated upon the first ET, is in competition with a second ET. A similar result was also observed from the decarboxylation of the phenylacetoxyl radical from the chemically-initiated ET reduction of phenylacetyl peroxide.[66]

The mass balance of phenyl-derived products is modest with the accounted mass typically around 75% (range 60–80%). The product loss is likely a consequence of the need to remove the electrolyte from the electrolysis mixture before quantifying by GC. In the heterogeneous electrolysis of DMPP, modest yields of MPPOH were also obtained so the unaccounted mass in the homogeneous studies is undoubtedly from unrecovered

Table 3 Homogeneous product studies of DMPP with electrochemically generated radical anion donors in acetonitrile–0.10 M TEAP solution. Yields are expressed in mole % based on consumption of DMPP[a]

Donor	Anthracene	DPA	Fluoranthene	Perylene	4m4mAzo	Azobenzene
$E°$/V	−1.965	−1.873	−1.762	−1.674	−1.478	−1.335
n	2.0	2.2	1.9	2.1	2.0	—
Donor recovered	95[b,c]	100[d]	100[b,d]	80[d]	65[b]	50[b]
MPPOH	115	122	124	105	90	50
Toluene	32	36	30	27	25	3
Bibenzyl	< 1	< 1	< 1	< 1	< 1	4

[a] No DMPP was recovered in all experiments. Amount of donor recovered quantified by [b] gas chromatography, [c] ^{1}H NMR, and [d] cyclic voltammetry. All other yields quantified by gas chromatography. DPA = diphenylanthracene; 4m4mazo = 4-methyl-4′-methoxyazobenzene.

Table 4 Homogeneous product studies of BMPP with electrochemically generated radical anion donors in acetonitrile–0.10 M TEAP solution. Yields are expressed in mole % based on consumption of BMPP[a]

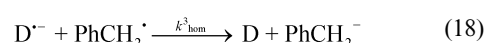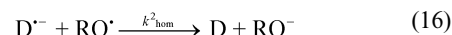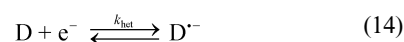| Donor	Anthracene	DPA	Fluoranthene	Perylene	4m4mAzo	Azobenzene
$E°$/V	−1.965	−1.873	−1.762	−1.674	−1.478	−1.335
n	2.0	2.0	1.8	2.0	—	—
Donor recovered	91[b,c]	100[d]	100[b,d]	80[d]	56[b]	44[b]
MPPOH	53	57	49	51	44	50
Toluene	17	18	12	13	8	7
Bibenzyl	0	0	0	< 1	< 1	2

[a] Unreacted BMPP was recovered in the experiments with 4m4mazo and azobenzene in 57 and 84% yield. Amount of donor recovered quantified by [b] gas chromatography, [c] ^{1}H NMR, and [d] cyclic voltammetry. All other yields quantified by gas chromatography. DPA = diphenylanthracene; 4m4mazo = 4-methyl-4′-methoxyazobenzene.

MPPOH. Despite the modest yields, comparison of the results for both peroxides reveals [MPPOH]/[toluene] is approximately constant with a ratio of 3.7 to 1 for donors with $E° < −1.5$ V.

In contrast, with 4-methoxy-4′-methylazobenzene and azobenzene the amount of donor recovered is no greater than 65%. Comparison of the voltammetry of the redox couple before and after the reaction revealed a significant decrease in the mediator anodic current. MPPOH and toluene were still the major products; however, the amount of toluene decreases as the reduction potential of the donor becomes less negative with ratios of MPPOH to toluene as high as 17. With these two donors, GC analysis also revealed other signals at later retention times. These are attributed to products resulting from the destruction of the radical anion catalyst coupling with the benzyl radical.[63] From the studies with azobenzene two coupling products were characterised by GC/MS with m/z of 272. No coupling products were identified from the addition reaction between the radical anion and the alkoxyl radicals. Alkoxyl radicals have reduction potentials of ∼ −0.2 V so with all the donors used in this study reduction, rather than coupling, is the more favourable pathway.[37,38]

Having established the products from the indirect electrolysis, the dissociative mechanism of DMPP and BMPP can be adequately described by equations (14) through (20). After reduction of the aromatic donor to the radical anion (eqn. (14)) the peroxide is reduced in a concerted ET (eqn. (15)) to yield an alkoxyl radical, which can be subsequently reduced by another radical anion molecule (eqn. (16)), or in the case of the MPPH alkoxyl radical, rapidly undergoes the β-scission fragmentation (eqn. (17)). The *tert*-butoxyl radical will react by reduction since its β-scission fragmentation is considerably slower (8.3×10^4 s^{-1}).[67] Upon fragmentation of the MPPH alkoxyl radical, acetone and a benzyl radical are liberated (eqn. (17)). The benzyl radical in the presence of a radical anion donor reacts competitively either by reduction (eqn. (18)) or coupling with the donor (eqn. (19)) as previously reported.[63,68,69] Dimerization of the benzyl radical (eqn. (20)) is a minor side reaction in comparison to eqns. (18) and (19) as only a trace amount of bibenzyl is observed on work-up, a testament to the low steady-state concentration of the benzyl radical. Applying the method of homogeneous redox catalysis,[70–73] kinetics for dissociative electron transfer, k^1_{hom} (eqn. (15)), can be accurately evaluated once all the other rate constants for eqns. (14) through (20) are known. Besides k^1_{hom}, the only other rate constant not known with certainty is k^3_{hom}. It was estimated by examining the competition kinetics between eqns. (18) and (19) as described in the next section.

$$D + e^- \underset{}{\overset{k_{het}}{\rightleftarrows}} D^{\bullet -} \qquad (14)$$

$$D^{\bullet -} + ROOR \xrightarrow{k^1_{hom}} D + RO^\bullet + {}^-OR \qquad (15)$$

$$D^{\bullet -} + RO^\bullet \xrightarrow{k^2_{hom}} D + RO^- \qquad (16)$$

$$RO^\bullet \xrightarrow{k_\beta} PhCH_2^\bullet + CH_3COCH_3 \qquad (17)$$

$$D^{\bullet -} + PhCH_2^\bullet \xrightarrow{k^3_{hom}} D + PhCH_2^- \qquad (18)$$

$$D^{\bullet -} + PhCH_2^\bullet \xrightarrow{k_c} DPhCH^- \qquad (19)$$

$$2\,PhCH_2^\bullet \xrightarrow{k_{dim}} PhCH_2CH_2Ph \qquad (20)$$

q Parameter measurements and the determination of k^3_{hom}

The competition between the homogeneous ET (eqn. (18)) and coupling between a radical anion donor and the benzyl radical (eqn. (19)) can be expressed by the dimensionless parameter q:

$$q = \frac{k^3_{hom}}{k^3_{hom} + k_c} \qquad (21)$$

In the case $k^3_{hom} \gg k_c$, the major pathway is an ET and q is equal to 1.0. In the scenario where $k_c \gg k^3_{hom}$ only coupling between the radical and radical anion donor is observed and q equals 0.0. A value of q in between these two extremes ($0.0 < q < 1.0$) indicates a partitioning between the two processes. Numerous studies with various carbon radicals including alkyl,[74,75] allyl[75] and acyl,[76] have demonstrated the competition between eqns. (18) and (19) is related to the potential difference between the redox potential of the donor, $E°_{D/D^{\bullet -}}$, and of the radical, in our case, the benzyl radical, $E°_{PhCH_2^\bullet/PhCH_2^-}$.[77]

Table 5 Competition q parameters for the reactivity of the benzyl radical with radical anion donors determined by the RDE and ultramicroelectrode method in 0.10 M TEAP–DMF solution

Donor	q^a	k^3_{hom}/M^{-1} s$^{-1 b}$
Fluoranthene	0.95	1.9×10^{10}
Perylene	0.85	5.7×10^9
Tetracene	0.70	2.3×10^9
4m4mazo^c	0.40	6.7×10^8
4-Methoxyazobenzene	0.15	1.8×10^8
Azobenzene	0.00	$1.0 \times 10^{7 d}$

^{a} Determined according to K. Daasbjerg, *Acta Chem. Scand.*, 1993, **47**, 398–402. ^{b} Calculated from the measured q-value and eqn. (21) with $k_c = 1 \times 10^9$ M^{-1} s^{-1}. ^{c} 4-Methyl-4′-methoxyazobenzene. ^{d} Calculated using $q = 0.01$.

Studies with radical probes,[78,79] and most recently by a laser flash photolysis method,[80] indicate $k_c = 1 \times 10^9$ M^{-1} s^{-1} is a reasonable approximation for coupling between aromatic radical anions and alkyl and benzyl radicals independent of the standard potential of $E°_{D/D^{\cdot-}}$. Thus, eqn. (21) provides a way of evaluating k^3_{hom} once q is known. Most q parameter studies have utilised linear sweep voltammetry as the technique of choice, as has been done with a number of benzylic-like radicals.[77,81] We have measured the competition q-values for our series of donors using the rotating disk electrode (RDE) and ultramicroelectrode method.[76,82] This relatively unused technique has many advantages over linear sweep voltammetry including a more accurate determination of q, and can be used for slow reactions with a rate constant as low as 10^{-3} M^{-1} s^{-1}.[82]

The q-values were measured in N,N-dimethylformamide from the average of several experiments with DMPP as the substrate. They are reported in Table 5 along with the values of k^3_{hom}. The trend observed with the q-values parallels the results from the homogeneous product studies in Tables 3 and 4. For example, in the product studies with fluoranthene no loss of the mediator was observed by GC or cyclic voltammetry so q with this donor is 1.0. A q-value of 0.95 was experimentally measured, which is within the error limit of the RDE and ultramicroelectrode techniques. As the reduction potential of the donor becomes more positive than fluoranthene, q is found to decrease towards zero in accordance with the lower recovery yields of donor in the product studies.

In Fig. 2, the q-values are plotted as a function of $E°_{D/D^{\cdot-}}$. The plot exhibits an S-shaped curve with q decreasing with increasing $E°_{D/D^{\cdot-}}$. A rigorous non-linear regression analysis was used to extract the standard reduction potential of the benzyl radical. Interpolation of the plot allows for the determination of the half-wave potential, $E^q_{1/2}$, which is the
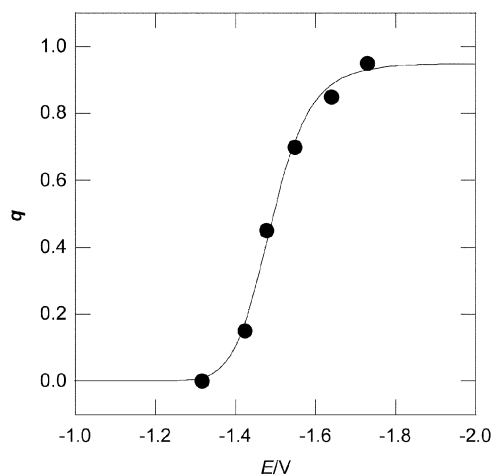
Fig. 2 The competition parameter q for the benzyl radical as a function of the $E°_{D/D^{\cdot-}}$ of aromatic donors. The data were acquired with DMPP as the substrate in DMF–0.10 M TEAP solution.

$E°_{D/D^{\cdot-}}$ of the donor where $k^3_{hom} = k_c$ and $q = 0.5$. The curve fitting analysis of the data is based on the quadratic-activation relationship described by the Marcus theory of ET accounting for diffusion (eqn. (22)):[83]

$$k^3_{hom} = \frac{k_d}{1 + \dfrac{k_d}{K_d Z}\exp\left[\dfrac{\lambda}{4RT}\left(1 + \dfrac{\Delta G_{ET}}{\lambda}\right)^2\right] + \exp\left(\dfrac{\Delta G_{ET}}{RT}\right)} \quad (22)$$

where k_d is the diffusion-limited rate constant, K_d is the equilibrium constant for formation of the encounter complex, Z is the collision frequency for an adiabatic ET, λ is the reorganisation energy, and ΔG_{ET} is the free energy of the ET reaction. Substitution of eqn. (22) into eqn. (21) and $\Delta G_{ET} = 23.06$ ($E°_{D/D^{\cdot-}} - E°_{PhCH_2^{\cdot}/PhCH_2^-}$) yields an expression relating the q parameter as a function of $E°_{D/D^{\cdot-}}$:

$$q = \frac{1}{1 + \dfrac{k_c}{k_d}\left\{1 + \dfrac{k_d}{K_d Z}\exp\left[\dfrac{\lambda}{4RT}\left(1 + \dfrac{\Delta G_{ET}}{\lambda}\right)^2\right] + \exp\left(\dfrac{\Delta G_{ET}}{RT}\right)\right\}} \quad (23)$$

In the curve fitting analysis the following parameter values were used: $k_c = 1 \times 10^9$ M^{-1} s^{-1}, $Z = 3 \times 10^{11}$ M^{-1} s^{-1}, $K_d = 1$ M^{-1}, and $k_d = 2 \times 10^{10}$ M^{-1} s^{-1}. K_d was calculated from $K_d = (4/3)\pi a^3 N_a$, the expression for the stability constant of the encounter complex when at least one reagent is uncharged where a is the centre-to-centre distance between the reagents with radii of 3.5 Å. From the fit of the data $E°_{PhCH_2^{\cdot}/PhCH_2^-} = -1.49 \pm 0.03$ V and $\lambda = 13.4 \pm 1.5$ kcal mol^{-1}. These values for the standard reduction potential and the reorganisation energy are in excellent agreement with results from other techniques.[77,84,85]

Homogeneous kinetics

The outer-sphere ET kinetics from a series of electrochemically generated radical anion donors were measured for DMPP and BMPP in DMF using the methods of homogeneous redox catalysis[70–73] and a potentiometric technique using a rotating disk electrode.[86,87] In the first method, mediators were chosen with a reversible electron transfer couple (D/D$^{\cdot-}$) with both oxidised and reduced species stable on the voltammetric time scale, and the reduction potential of the donor positive to the peak potential of the peroxide. The reversible reduction wave of the radical anion donor, D$^{\cdot-}$, is monitored (eqn. (14)) as a function of peroxide concentration and sweep rate. As increasing concentrations of peroxide are added to the donor solution, the reversible wave of the donor is transferred into a chemically irreversible wave and the cathodic peak current increases catalytically (eqn. (15)). Based on eqns. (14)–(20) and known rate constants for the various steps, including the values of k^3_{hom} determined by the q method, ET rate constants for the O–O cleavage (k^1_{hom}) were determined by digital simulation. In the simulations of the unsymmetrical peroxide, BMPP, the fragments from dissociative ET were treated as different entities. A set of side reactions with DMF was also included in the analysis.[38,64]

The homogeneous kinetics (k^1_{hom}) measured by both techniques are summarised in Table 6. Spanning 6 orders of magnitude, the rate constants increase as the standard potential of the donor becomes more negative as a consequence of an increase in the driving force for ET expressed as $\Delta G_{ET} = 23.06$ ($E°_{D/D^{\cdot-}} - E°_{diss}$). The $E°_{D/D^{\cdot-}}$, reported in Table 6, were measured by cyclic voltammetry; the $E°_{diss}$ cannot be determined directly due to the irreversible nature of concerted ETs. However, $E°_{diss}$ can be estimated by at least two ways: (i) by convolution analysis as previously outlined and (ii) by a thermochemical cycle yielding eqn. (24).[38,88]

$$E°_{diss} = E°_{RO^{\cdot}/RO^-} - BDFE / F \quad (24)$$

Table 6 Rate constants for electron transfer from electrochemically generated radical anion donors to DMPP and BMPP measured in DMF–0.10 M TEAP solution at 25 °C

Donor	$E°_{D/D^{•-}}$ (DMF)[a]/ V vs. SCE	DMPP ΔG_{ET}/kcal mol^{-1}[b]	DMPP log (k^1_{hom}/M^{-1} s^{-1})	BMPP ΔG_{ET}/kcal mol^{-1}[c]	BMPP log (k^1_{hom}/M^{-1} s^{-1})
Isoquinoline	−2.158	—	—	−16.8	4.64[d]
Pyrene	−2.054	—	—	−14.4	4.37[d]
Anthracene	−1.934	−12.8	4.18[d]	−11.6	3.83[d]
Diphenylanthracene	−1.838	−10.6	4.04[d]	−9.4	3.56[d]
Fluoranthene	−1.730	−8.1	3.33[d]	−6.9	2.85[d]
Perylene	−1.641	−6.0	3.10[d]	−4.9	2.57[d]
Tetracene	−1.548	−3.9	2.04[d]	−2.7	1.62[d]
4-Methyl-4′-methoxyazobenzene	−1.478	−2.3	1.46[d]	−1.1	0.92[e]
4-Methoxyazobenzene	−1.423	−1.0	0.91[e]	0.2	0.34[e]
Azobenzene	−1.315	1.5	0.10[e]	2.7	−0.39[e]
3,3′-Dimethoxyazobenzene	−1.256	2.9	−0.15[e]	—	—
2-Nitrobiphenyl	−1.177	4.7	−1.32[e]	5.8	−1.39[e]
Nitrobenzene	−1.100	6.5	−1.30[e]	7.6	−1.70[e]
1-Nitronaphthalene	−1.035	8.0	−1.70[e]	9.1	−1.93[e]

[a] $E°$ measured in DMF versus ferrocene and corrected using $E°_{Fc/Fc^+}$ = 0.475 V. [b] ΔG_{ET} calculated from $E°_{DMPP}$ = −1.38 V. [c] ΔG_{ET} calculated from $E°_{BMPP}$ = −1.43 V. [d] Measured by homogeneous redox catalysis. [e] Measured by a method using a rotating disk electrode.

Determination of the $E°_{diss}$ requires knowledge of the bond dissociation free energy (BDFE), and the reduction potential for the alkoxyl radical, $E°_{RO^•/RO^-}$, where F is the Faraday constant (eqn. (24)). An estimate of the BDFE can be obtained from the literature bond dissociation enthalpies (BDE) of related peroxides and by including an entropy correction.[89] The value of $E°_{RO^•/RO^-}$ can be estimated from cyclic voltammetry measurements provided the effect for the kinetic peak shift is taken into account.[88] Accounting for the peak shift, $E°_{MPPO^•/MPPO^-}$ (ACN) = −0.20 V and $E°_{MPPO^•/MPPO^-}$ (DMF) = −0.13 V vs. SCE. The standard potentials for the tert-butoxyl radical were previously reported to be $E°_{t-BuO^•/t-BuO^-}$ (ACN) = −0.30 V and $E°_{t-BuO^•/t-BuO^-}$ (DMF) = −0.23 V vs. SCE.[38] From eqn. (24) and the data provided here, the $E°_{diss}$ for both DMPP and BMPP are estimated to be within ± 0.10 V: $E°_{DMPP}$ (ACN) = −1.45 V, $E°_{DMPP}$ (DMF) = −1.38 V, $E°_{BMPP}$ (ACN) = −1.50 V, and $E°_{BMPP}$ (DMF) = −1.43 V vs. SCE.[90]

Likewise the thermochemical approach can be used to evaluate the standard reduction potential of 2-methyl-1-phenyl-2-propyl hydroperoxide, $E°_{MPPH}$. The BDE of hydroperoxides are slightly larger than dialkyl peroxide ranging from 40 to 50 kcal mol^{-1}. The BDE of MPPH was estimated from the heats of formation for the homolytic cleavage of the O–O bond to be 44.8 kcal mol^{-1}.[91,92] Applying the same methodology, $E°_{MPPH}$ (DMF) = −1.70 V, and $E°_{MPPH}$ (ACN) = −1.77 V.

Discussion

Analysis of the kinetics

Knowing the values of $E°_{DMPP}$ and $E°_{BMPP}$, the ΔG_{ET} can be accurately calculated and plotted versus log (k^1_{hom}) as shown in Figs. 3a and 3b. The data are fit to a form of the Marcus expression derived for dissociative ET,[52–54] which relates the activation free energy, $\Delta G^{\neq}$, to the reaction free energy, ΔG_{ET}, and to the Eyring expression (eqn. (25)). Savéant's expression is similar to the Marcus equation (eqn. (26)) with the exception that the intrinsic barrier, $\Delta G_0^{\neq}$, contains contributions from the BDE of the cleaving bond (in this case the O–O bond) in addition to the reorganisation energy, λ (eqn. (27)). Savéant's theory, originally applied to alkyl halides, assumed ET is adiabatic where the transmission coefficient, κ, is equal to 1 and the pre-exponential factor, Z, is approximately 3×10^{11} M^{-1} s^{-1}. Previous studies by our group and Maran and co-workers have revealed that ET to peroxides and endoperoxides is non-adiabatic,[37,38,44] where $\kappa \ll 1$, on the order of 0.01 to 0.02.[38]

Using Savéant's dissociative ET theory, two parameters can be extracted directly from the homogeneous kinetic data, $\Delta G_0^{\neq}$
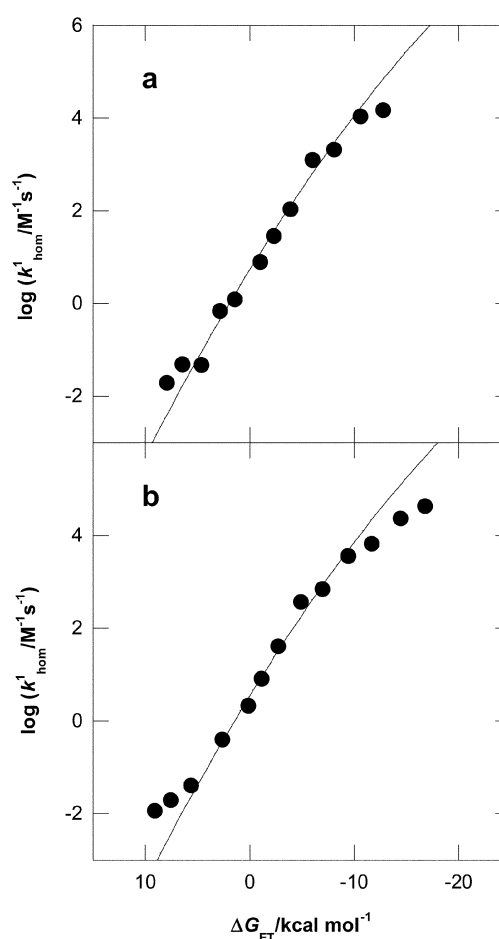

Fig. 3 The homogeneous rate constants for reduction of (a) DMPP and (b) BMPP measured by redox catalysis and chronopotentiometry. The solid line through the data is the best fit according to eqns. (25) and (26) with $\Delta G_0^{\neq}$ = 13.0 kcal mol^{-1} and a non-adiabatic log (κZ_{hom}) term.

$$k_{ET} = \kappa Z \exp\left(-\frac{\Delta G^{\neq}}{RT}\right) \quad (25)$$

$$\Delta G^{\neq} = \Delta G_0^{\neq}\left(1 + \frac{\Delta G_{ET}}{4\Delta G_0^{\neq}}\right)^2 \quad (26)$$

$$\Delta G_0^{\neq} = \frac{BDE + \lambda}{4} \quad (27)$$

and κZ_{hom}. The intrinsic barrier (eqn. (27)) was determined using an average BDE of 37 kcal mol^{-1}, typical of dialkyl peroxides, and a calculated λ using a previously documented approach.[37,38] Estimates for λ can be determined using expressions by Marcus, Kojima–Bard and Savéant and the radius of the donor, r_{D}, and the radius of the peroxide acceptor, r_{AB}.[93] With the Bard approach, $\lambda = 95[(2r_{\mathrm{D}})^{-1} + (2r_{\mathrm{AB}})^{-1} - (r_{\mathrm{D}} + r_{\mathrm{AB}})^{-1}]$, the λ's are 14.9 and 14.8 kcal mol^{-1} and $\Delta G_0^{\ne} = 13.0$ kcal mol^{-1} for both peroxides. This value for the intrinsic barrier was used to provide reasonable estimates of $\log(\kappa Z_{\mathrm{hom}})$ by a curve fitting analysis of the homogeneous kinetics. As seen in Figs. 3a and 3b, the curve fits are parabolic as predicted by the theories of ET. The fit of the log (k^1_{hom}) *versus* ΔG_{ET} plot gives values of $\log(\kappa Z_{\mathrm{hom}}) = 10.3 \pm 0.1$ for DMPP and $\log(\kappa Z_{\mathrm{hom}}) = 10.1 \pm 0.1$ for BMPP. Removing the data points at the slowest end from the best fit of the BMPP kinetics has a minimal effect on the extracted parameters. However, if ET to the peroxides was assumed to be adiabatic ($\kappa = 1$) and log ($Z_{\mathrm{hom}}) = 11.7$[94] then $\Delta G_0^{\ne} = 15$ kcal mol^{-1}. With an estimated λ of 14.9 kcal mol^{-1}, the BDE would be 46 kcal mol^{-1}, which is significantly larger than the accepted BDE of dialkyl peroxides. A comparison between the theoretical adiabatic pre-exponential factor and the determined non-adiabatic value reveals a discrepancy ranging from 1.4 to 1.6 orders of magnitude. The effect of steric hindrance on ET to the σ^* orbital was found to contribute 0.8 log units, estimated from comparison of the heterogeneous reduction of di-*tert*-butyl peroxide with di-*n*-butyl peroxide.[38] However, if an E°_{diss} value of 0.1 V more positive is used to calculate the ΔG_{ET}, an average between the thermochemical and convolution determined E°_{diss}, log (κZ_{hom}) decreases by 0.8 log units. But given the error in E°_{diss}, the pre-exponential factors determined from the curve fitting analysis are consistent with the results obtained from the temperature dependence study of di-*tert*-butyl peroxide.[38]

Recently, Savéant has addressed the analysis of the heterogeneous activation-driving force data by a quadratic expression.[95] Equation (25) is still valid, but eqn. (26) includes a proportionality factor of 1.07 in the intrinsic barrier. A similar curve fitting analysis was performed with the heterogeneous kinetics obtained from the convolution analysis as shown in Figs. 4a and 4b.

The heterogeneous kinetics was related to ΔG_{ET} using the reported E°_{diss} in Table 2. Reasonable values were extracted by fitting for both $\Delta G_0^{\ne}$ and log (κZ_{het}) simultaneously. For DMPP and BMPP, the intrinsic barriers were evaluated to be 10.7 ± 0.1 and 11.4 ± 0.1 kcal mol^{-1}, similar to the values reported in Table 2, and the log (κZ_{het}) are -0.46 ± 0.01 and -0.14 ± 0.01, respectively. Using the thermochemical E°_{diss} to calculate ΔG_{ET} has the effect of lowering $\Delta G_0^{\ne}$ no more than 1 kcal mol^{-1} and log (κZ_{het}) by only 0.3 log, while setting log (κZ_{het}) to the adiabatic value 3.6,[96] yields a poor fit with a $\Delta G_0^{\ne}$ of 17 kcal mol^{-1}. The experimentally determined log (κZ_{het}) and the heterogeneous adiabatic log (Z) differ by at least 3.7 log units, again suggesting the ET is non-adiabatic. The greater difference in the experimental log (κZ_{het}) from the adiabatic value, in comparison to the homogeneous data, may be due to the heterogeneous data covering a narrower driving force range. It is also possible that a distance effect because of the diffuse double layer at the electrode interface may also contribute to a lower heterogeneous pre-exponential factor. As for the evaluation of λ, eqn. (27) yields values ranging from 6 to 9 kcal mol^{-1} whereas including the proportionality factor of 1.07 yields values 3 kcal mol^{-1} lower.

Determination of k^2_{het}

From the heterogeneous product analysis and from the simulated concentration profiles, qualitatively we can conclude that the second heterogeneous ET to the alkoxyl radical occurs at a rate much faster than the rate of β-scission fragmentation with
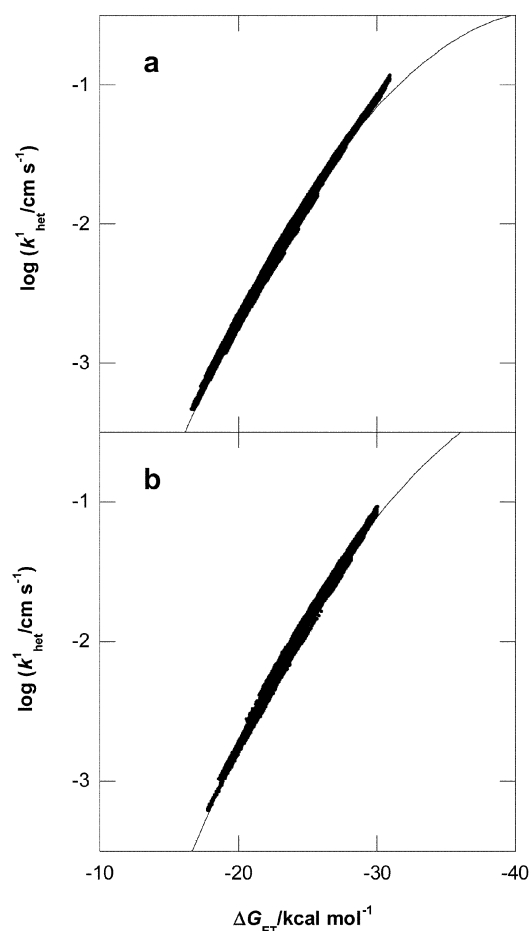

Fig. 4 The heterogeneous rate constants for reduction of (a) DMPP and (b) BMPP measured by convolution analysis. The solid line through the data is the best fit according to eqns. (25) and (26) with a $\Delta G_0^{\ne}$ and a non-adiabatic log (κZ_{het}) term as described in the text.

a rate constant of 2.2×10^8 s^{-1}. Recall from Scheme 1 that both parallel competing reactions are irreversible so the rate constant ratio is equal to the ratio of the product yields [MPPOH]/[toluene] provided the contributions from the following chemistry (protonations) are negligible. Based on the heterogeneous electrolysis studies, we showed the ratio of MPPOH to toluene produced after ET is in excess of 100 to 1. Equating the product ratio to the rate constant ratio, and from the knowledge of k_β, *and by accounting for the diffuse double layer at the electrode interface*, an inherent property of heterogeneous ETs, k^2_{het} can be calculated and expressed as a rate constant in units of cm s^{-1}.

The distance dependence at the electrode interface is accounted for using the Gouy-Chapman model of the diffuse double layer.[56] The model postulates that ET occurs at the closest possible distance to the electrode, that being the outer Helmholtz plane. For solutions of ACN and DMF with a relative permittivity equal to 37 at 25 °C, the expression $\kappa = 4.79 \times 10^7 z C^{*\frac{1}{2}}$ can be used to characterise the thickness of the diffuse layer, where z is the charge magnitude of each ion of the electrolyte, C^* is the bulk electrolyte concentration in mol L^{-1} and κ is given in cm^{-1}.[56] The reciprocal of κ is a measure of the diffuse double layer thickness. For a 0.10 M TEAP solution, κ is calculated to be 6.6×10^{-8} cm. Therefore, the product of κ and the value extracted from the competition kinetics yields k^2_{het} equal to 1500 cm s^{-1}. Incidentally, the driving force for reduction of the alkoxyl radical is thermodynamically favourable, based on the potential difference between the peroxide peak potential and the reduction potential of the alkoxyl radicals, in excess of 1.8 V or 41 kcal mol^{-1}.

Conclusions

Electron transfer to O–O bonds is inherently slow, although the peroxide bond is weak. Even for a highly driven ET, one must consider that other chemical processes may be able to compete. A comparison of the structurally related dialkyl peroxides, dicumyl and di-*tert*-butyl peroxide, reveals the thermochemical parameters and kinetics are similar[38,58] to those for the peroxides in this study, which is clearly evident when the kinetics of each are plotted together. The significant difference with DMPP and BMPP from their predecessors is in the follow-up chemistry after cleavage of the O–O bond on accepting an electron from a homogeneous donor. Heterogeneously, only reduction of the MPPH alkoxyl radical was observed; homogeneously, a competition was observed between reduction and β-scission followed by a second competition involving the benzyl radical, which was characterised from product analysis and by evaluating the competition q parameter. DMPP and BMPP were primarily devised as kinetic probes to investigate the rate constant of the heterogeneous ET to alkoxyl radicals (k^2_{het}) liberated by DET. Now, with a thorough understanding of the ET chemistry of DMPP and BMPP, these peroxides can be used as mechanistic probes for the occurrence of DET. Studies utilizing these peroxides as mechanistic probes are currently in progress. Aspects of the knowledge gained from this study should assist those employing MPPH as a mechanistic probe by providing more predictability power with a better understanding of kinetics and thermodynamics.

Experimental

Materials

Spectroscopic grade *N,N*-dimethylformamide was distilled over CaH$_2$ under a nitrogen atmosphere at reduced pressure. Spectroscopic acetonitrile was fractionally distilled over CaH$_2$ under a nitrogen atmosphere. The distilled solvents were stored in glass bottles under an inert atmosphere in the dark. The supporting electrolyte, tetraethylammonium perchlorate (TEAP), was recrystallized three times from ethanol and stored under vacuum. The aromatic donors pyrene, anthracene, diphenylanthracene, fluoranthene, perylene, and 1-nitronaphthalene were of high purity and used as received. Isoquinoline and nitrobenzene were distilled prior to use. Tetracene and 2-nitrobiphenyl were recrystallised from ethanol. 4-Methoxy-4′-methylazobenzene and 4-methoxyazobenzene were synthesised from the corresponding hydroxy-substituted azobenzene by reaction of methyl iodide with potassium carbonate in acetone and recrystallised. 4-Hydroxy-4′-methylazobenzene[97] and 3,3-dimethoxyazobenzene[98] were prepared by literature procedures. Trifluoroethanol was distilled, acetanilide was recrystallised from water, and ferrocene sublimed prior to use. All solvents and reagents not specified were used without purification and are available from Aldrich. Flash chromatography was performed with silica gel 60 (230–400 mesh ASTM) and fractions developed in hexanes on Kieselgel 60 F$_{254}$ TLC plates.

Instrumentation

Nuclear magnetic resonance spectra were recorded on a Varian Mercury spectrometer. ^{1}H and ^{13}C NMR spectra were recorded at 400.1 and 100.6 MHz, respectively, with CDCl$_3$ as the solvent and are reported in ppm *versus* tetramethylsilane ($\delta = 0.00$) for ^{1}H NMR and CDCl$_3$ ($\delta = 77.00$) for ^{13}C NMR. Infra-red spectra were recorded neat on a Bomem MB 100 FT-IR spectrometer between NaCl plates. Mass spectrometry was performed on a MAT 8200 Finnigan high resolution mass spectrometer. GC/MS spectra were obtained with a Varian Saturn 2000 GC/MS/MS interfaced to a Varian CP 3800 gas chromatograph with a CD-Sil 5 CB-MS 30 m × 0.25 mm

capillary column. Product studies were quantified on a Hewlett Packard 5890 Series II gas chromatograph interfaced to an HP 3393A integrator with a 14 m × 0.32 mm × 0.25 μm HP 50+ capillary column. The densities of the peroxides were determined from the mass of a known volume on an analytical balance in a tared 10 μL Hamilton syringe. The syringe was calibrated using 99+% hexadecane with a density of 0.773 g mL^{-1}. The estimated error on the density measurements is 4% by the least-squares method.

Synthesis

Caution. *Although no problems were encountered, dialkyl peroxides and alkyl hydroperoxides are potentially explosive.* Syntheses were performed in a fumehood behind a safety shield. The syntheses of di-2-methyl-1-phenyl-2-propyl peroxide (DMPP) and *tert*-butyl 2-methyl-1-phenyl-2-propyl peroxide (BMPP) were performed using a literature procedure with some modifications[99] by reacting 2-methyl-1-phenyl-2-propyl bromide with the required hydroperoxide and silver trifluoroacetate. 2-Methyl-1-phenyl-2-propyl bromide was synthesised from 2-methyl-1-phenyl-2-propanol with concentrated HBr and LiBr.[100] 2-Methyl-1-phenyl-2-propyl hydroperoxide (MPPH) was synthesised from 2-methyl-1-phenyl-2-propanol using 50% hydroperoxide and concentrated sulfuric acid[101] and from 2-methyl-1-phenyl-2-propyl bromide.[99] The crude dialkyl peroxide mixtures were subjected to NaBH$_4$ in methanol to reduce the major side product trifluoroacetic acid 1,1-dimethyl-2-phenylethyl ester (identified by ^{1}H, ^{19}F, IR, MS and has a reduction potential of -2.39 V *vs.* SCE at 0.1 V s^{-1}), simplifying purification by flash chromatography.

tert-**Butyl 2-methyl-1-phenyl-2-propyl peroxide (BMPP).** To an oven-dried 100 ml 2-neck round-bottom flask containing a 1″ magnetic stir bar and immersed in an ice bath, 2-methyl-1-phenyl-2-propyl bromide (5.0 g, 23 mmol) was added. *tert*-Butyl hydroperoxide (2.5 g, 28 mmol), dried over Na$_2$SO$_4$, was then added to the flask in slight excess followed by 20 mL of pentane. Silver trifluoroacetate (5.3 g, 24 mmol) was added in 500 mg portions to the solution with stirring over a 30 min period and the reaction mixture stirred for 2 hours. The heterogeneous mixture was filtered into a 125 ml separatory funnel. The solution was washed 3 times with 20 ml of water, dried over Na$_2$SO$_4$, and the solvent removed by a rotary evaporator to give a crude mixture with BMPP in 65% yield by ^{1}H NMR. The mixture was subjected to NaBH$_4$ in MeOH to reduce the trifluoroester product to the reagent alcohol (MPPOH). One mole equivalent of NaBH$_4$ to trifluoroester product was used. The solution was allowed to stir immersed in an ice bath for 1 hour. Afterwards 10 ml of 5% acetic acid were added to the solution, which was stirred for an additional 15 minutes, and then extracted 4× with 15 ml portions of CH$_2$Cl$_2$, washed 3× with 20 mL of water, dried over Na$_2$SO$_4$ and the solvent removed by a rotary evaporator. BMPP was purified and separated on silica gel (1 : 100 ratio) by flash chromatography using 2% ethyl acetate–98% petroleum ether (30–60 °C) in an overall yield of 50%. Clear, colourless liquid, density 1.01 g mL^{-1}; UV-vis (CH$_3$CN): $\lambda_{max} = 210$ nm, $\varepsilon = 8500$ M^{-1} cm^{-1}, $\lambda_{max} = 258$ nm, $\varepsilon = 200$ M^{-1} cm^{-1}; ν_{max}(NaCl)/cm^{-1} 3064, 3029 (=C–H), 2977, 2933 (C–H), 1603 (C=C), 1198 (C–O), 871 (O–O); ^{1}H NMR (CDCl$_3$): δ 1.16 (s, 6H), 1.23 (s, 9H), 2.84 (s, 2H), 7.16–7.27 (m, 5H); ^{13}C NMR (CDCl$_3$): δ 24.55, 26.68, 45.39, 78.51, 80.42, 125.95, 127.66, 130.68, 138.25; MS/EM found 222.162, calculated 222.162: m/z(intensity): 222(4), 131(29), 91(100), 73(75), 57(19).

Di-2-methyl-1-phenyl-2-propyl peroxide (DMPP). To an oven-dried 100 ml 2-neck round-bottom flask containing a 1″ magnetic stir bar and immersed in an ice bath 2-methyl-1-phenyl-2-propyl bromide (1.8 g, 8.4 mmol) and MPPH (1.4 g, 8.4 mmol) were added. To the flask was added approximately

20 mL of pentane. Silver trifluoroacetate (1.5 g, 7.0 mmol) was added in 500 mg portions to the solution over a 15 min period and the reaction mixture stirred for 3 hours. The work-up procedure was the same as described for BMPP. DMPP was separated and purified on silica gel (1 : 100 ratio) by flash chromatography using petroleum ether (30–60 °C) in an overall yield of 30%. Pale yellow oil, density 1.13 g mL^{-1}; UV-vis (CH$_3$CN): λ_{max} = 210 nm, ε = 23000 M^{-1} cm^{-1}, λ_{max} = 258 nm, ε = 370 M^{-1} cm^{-1}; ν_{max}(NaCl)/cm^{-1} 3063, 3029 (=C–H), 2978, 2934 (C–H), 1603 (C=C), 866 (O–O); ^{1}H NMR (CDCl$_3$): δ 1.18 (s, 12H), 2.87 (s, 4H), 7.17–7.28 (m, 10H); ^{13}C NMR (CDCl$_3$): δ 24.60, 45.60, 80.81, 126.01, 127.69, 130.72, 138.13; MS/EM found 298.193, calculated 298.193: m/z(intensity): 298(1), 207(4), 149(8), 117(9), 91(100), 65(5).

Electrochemical procedures

Cyclic voltammetry was performing using a Perkin-Elmer PAR 283 or 263A potentiostat interfaced to a personal computer with PAR 270 electrochemistry software. Experiments were performed using a three electrode arrangement placed in a water-jacket cell. A routine experimental setup is as follows: the cell stored in an oven at 110 °C was placed in a copper Faraday cage and purged with a continuous flow of high purity argon and connected to a cooling bath maintained at 25 °C throughout the entire experiment. The electrolyte, TEAP, was added to the cell followed by 25 mL of the appropriate solvent and a ½″ magnetic stir bar. The solution was bubbled with argon to expel oxygen from the solution.

The working electrode was a 3 mm diameter glassy carbon rod (Tokai, GC-20) sealed in glass tubing. Prior to use it was polished on a polishing cloth with diamond paste, rinsed and sonicated in 2-propanol for 10 min and finally dried with a stream of cool air. The working electrode was activated by cycling 25 times between 0 and −2.8 V $vs.$ SCE at a scan rate of 0.2 V s^{-1}. The counter electrode was a 1 cm^2 Pt plate. The reference electrode was a silver wire immersed in a glass tube with a sintered end containing 0.10 M TEAP in the relevant solvent. After each experiment, it was calibrated against the ferrocene/ferricenium couple. In 0.10 M TEAP, the $E°$ was taken to be 0.475 and 0.449 V $versus$ KCl saturated calomel electrode (SCE) in DMF and ACN, respectively.

The standard reduction potentials of the homogeneous donors were determined in a standard cell at several scan rates between 0.1 and 2.0 V s^{-1} using 1–5 mM concentrations of donor. Afterwards, 1–3 mM ferrocene was added to the cell and a series of cyclic voltammograms at identical sweep rates were acquired. The standard potentials of ferrocene and the aromatic donors were taken as the midpoint between the anodic and cathodic peak potentials.

Heterogeneous product studies

Constant potential electrolyses were performed with a Perkin-Elmer PAR 263A potentiostat using the same cell setup as mentioned previously with the following exceptions: the working electrode was an EDI101 RDE electrode with a 12 mm tip (or a platinum foil) and the counter electrode was a platinum wire immersed in a glass frit containing a 2 mm layer of neutral alumina. A 3 mm glassy carbon electrode was used to probe the concentration of peroxide. After cell setup, the electrolyte solution was pre-electrolysed at a potential over 100 mV negative to the peroxide reduction peak potential. The experiments were performed at approximately 100 mV negative to the peak potential of the peroxide and continued until less than 3% of the initial peak current remained. In some cases, the electrolysis was continued until the initial peak current was reduced to the initial background. The electron count was typically 2.0 ± 0.2. Once the electrolysis was complete, dilute acetic acid or water (10 mL) was added to the cell and the contents extracted with dichloromethane (4 × 10 mL). The organic extract was washed

(5–12 times) with water (20mL), more so when DMF was the electrochemical solvent. At times, brine was added to break up emulsions. An aliquot of the organic extract was analysed by GC. The remaining solution was dried over sodium sulfate, filtered and the solvent evaporated and the mass balance measured. For DMPP only one product was recovered: 2-methyl-1-phenyl-2-propanol (MPPOH) in 65% yield. ^{1}H and ^{13}C NMR, and GC/MS were in agreement with those of an authentic sample. ^{1}H NMR (CDCl$_3$, ppm): δ 1.23 (s, 6H), 1.39 (s, broad, 1H), 2.77 (s, 2H), 7.18–7.30 (m, 5H); ^{13}C NMR (CDCl$_3$, ppm): 29.26, 49.75, 70.74, 126.34, 128.06, 130.29, 137.53. From product studies of BMPP, $tert$-butyl alcohol was detected by ^{1}H NMR as a singlet at 1.26 ppm. GC analysis of the cell contents before work-up revealed no toluene. Electrolyses were performed at least twice with each peroxide in each solvent with minimum concentrations of 2 mM.

Homogeneous product studies

The cell setup was identical to the heterogeneous product studies with the exception that a platinum foil was used for the bulk electrolysis. Initially, 1–2 mM solution of mediator was prepared and the reversible couple probed. Peroxide was added to make a 2 mM concentration and the solution probed again revealing an irreversible donor wave. The electrolysis was conducted at approximately 100 mV past the cathodic peak potential of the donor. The reaction was probed by cyclic voltammetry and halted after disappearance of the peroxide dissociative wave or after the catalytic wave of the donor was once again completely reversible (I_c/I_a = 1). The electron count was typically 2.0 ± 0.2. Once the electrolysis was complete, 10 ml of water were added to the cell. The contents were extracted with dichloromethane (3 × 8 mL) and washed 3 times with water or brine (10 mL). The organic extract was dried over sodium sulfate and filtered into a 25 mL volumetric flask. The volume was topped-off and pentadecane added as an internal standard. The sample was analysed by GC using calibration curves consisting of a minimum of 5 points. Injections were performed 2 or 3 times and found to be reproducible within 5%. The temperature program was as follows: 30 °C for 3 min, ramp 10 °C min^{-1} to 250 °C for 10 min at a flow rate of 90 mL min^{-1}. In some cases, the sample was also analysed by GC/MS and ^{1}H NMR (after evaporation). Identified in the reaction between azobenzene and DMPP were two coupling products between azobenzene and a benzyl radical: m/z(intensity): (isomer 1) 272(95), 195(7), 167(100), 165(34), 152(29), 105(11), 77(38); (isomer 2) 272(58), 195(100), 180(32), 165(33), 152(18), 77(21).

Kinetic measurements

Homogeneous rate constants were measured in DMF at 25 °C by two methods. The faster kinetics were measured using the set-up described above and the technique of homogeneous redox catalysis. A cyclic voltammograph of the reversible couple of the donor was recorded at 5–7 sweep rates between 0.1 and 2.0 V s^{-1} at 1 and 2 mM concentrations of donor in the absence of peroxide. Afterwards, measurements were performed with at least 3 different concentrations of peroxide with excess factors (the concentration ratio of peroxide to donor) ranging from 0.5 with the most catalytic donors up to values of 20 with the least catalytic. Peak ratios were determined from the cathodic peak current in the presence of peroxide relative to the initial peak current in the absence of peroxide. The voltammetric behaviour of the donor peak currents was then simulated using digital simulation software (Digisim 3.0 software by Bioanalytical Systems Inc.). Kinetic measurements with each peroxide were performed 2 or 3 times.

The slower kinetics were measured using a 3 mm rotating disk electrode to monitor the decay of donor radical anion upon addition of peroxide. A donor solution of 3–5 mM was reduced at a Pt foil to generate a 1 mM solution of radical

anion (2.5 F mol^{-1} was added). The solution was stirred at 4500 rpm and the stability of the radical anion monitored at one minute intervals. While stirring, a greater than 10-fold excess of peroxide was added to the solution and the exponential decay of the anodic current was recorded for a minimum of one half-life. Rate constants were extracted from the slopes of $\ln(I)$ *vs.* time plots discarding the initial portion of the decay curve. The plots were linear with correlation coefficients greater than 0.99. The slope of the line corresponds to $-2k^1_{hom}[\text{ROOR}]$. Each measurement was performed 2 or 3 times.

Competition parameter *q* measurements

Measurements were performed using the technique developed by Kim Daasbjerg[82] using either an RDE or a microultra-electrode. The RDE was a Radiometer Copenhagen EDI101 with a 3 mm tip connected to a CTV 101 speed control unit. The microultraelectrode was a 10 μm Pt electrode from Autolab. A donor solution of 2–5 mM in DMF was prepared and vigorously purged with argon. A voltammogram was recorded using an RDE spinning at 4500 rpm or a 10 μm Pt microelectrode. The donor was subsequently reduced at a Pt foil to generate a 2–3 mM solution of radical anion (4.8–7.2 F mol^{-1} added). Afterwards, a series of voltammograms were taken at one minute intervals to ensure the radical anion was stable and no oxygen was present in the cell and then approximately 0.5 mM peroxide was added to the radical anion solution with stirring. Voltammograms were recorded at regularly timed intervals until no significant changes were observed after 3 consecutive scans. At the concentrations used, the fastest reactions were complete within seconds whereas those with azobenzene took approximately 8 minutes. Measurements were performed at least 3 times.

Acknowledgements

References

1 D. H. R. Barton and D. Doller, *Acc. Chem. Res.*, 1992, **25**, 504–512.
2 D. H. R. Barton and W. Chavasiri, *Tetrahedron*, 1994, **50**, 19–30.
3 (*a*) D. H. R. Barton, *Chem. Soc. Rev.*, 1996, 237–239; (*b*) D. H. R. Barton, *Synlett*, 1996, 229–230.
4 T. Kojima, R. A. Leising, S. Yan and L. Que, Jr., *J. Am. Chem. Soc.*, 1993, **115**, 11328–11335.
5 R. A. Leising, J. Kim, M. A. Pérez and L. Que, Jr., *J. Am. Chem. Soc.*, 1993, **115**, 9524–9530.
6 J. Kim, R. G. Harrison, C. Kim and L. Que, Jr., *J. Am. Chem. Soc.*, 1996, **118**, 4373–4379.
7 K. Chen and L. Que, Jr., *J. Am. Chem. Soc.*, 2001, **123**, 6327–6337.
8 K. Chen, M. Costas and L. Que, Jr., *J. Chem. Soc., Dalton Trans.*, 2002, **5**, 672–679.
9 D. T. Sawyer, A. Sobkowiak and T. Matsushita, *Acc. Chem. Res.*, 1996, **29**, 409–416.
10 (*a*) P. R. Ortiz de Montellano, *Cytochrome P450: Structure, Mechanism and Biochemistry*, Plenum Press, New York, 1995; (*b*) J. T. Groves, *J. Chem. Educ.*, 1985, **62**, 928–931.
11 (*a*) I. Schlichting, J. Berendzen, K. Chu, A. M. Stock, S. A. Maves, D. E. Benson, R. M. Sweet, D. Ringe, G. A. Petsko and S. G. Sligar, *Science*, 2000, **287**, 1615–1622; (*b*) D. G. Kellner, S.-C. Hung, K. E. Weiss and S. G. Sligar, *J. Biol. Chem.*, 2002, **277**, 9641–9644.
12 J. L. McLain, J. Lee and J. T. Groves, in *Biomimetic Oxidations Catalyzed by Transition Metal Complexes*, ed. B. Meunier, Imperial College Press, London, 2000, pp. 91–169.
13 B. Meunier, in *Biomimetic Oxidations Catalyzed by Transition Metal Complexes*, ed. B. Meunier, Imperial College Press, London, 2000, pp. 171–214.
14 Z. Hu and S. M. Gorun, in *Biomimetic Oxidations Catalyzed by Transition Metal Complexes*, ed. B. Meunier, Imperial College Press, London, 2000, pp. 269–307.
15 A. C. Rosenzweig and S. J. Lippard, *Acc. Chem. Res.*, 1994, **27**, 229–236.
16 M. Sono, M. P. Roach, E. D. Coulter and J. H. Dawson, *Chem. Rev.*, 1996, **96**, 2841–2887.
17 J. T. Groves and Y.-Z. Han, in *Cytochrome P450: Structure, Mechanism and Biochemistry*, 2nd edn., Plenum Press, New York, 1995, pp. 3–48.
18 R. A. Leising, R. E. Norman and L. Que, Jr., *Inorg. Chem.*, 1990, **29**, 2553–2555.
19 R. A. Leising, Y. Zang and L. Que, Jr., *J. Am. Chem. Soc.*, 1991, **113**, 8555–8557.
20 Y. Zang, J. Kim, Y. Dong, E. C. Wilkinson, E. H. Appelman and L. Que, Jr., *J. Am. Chem. Soc.*, 1997, **119**, 4197–4205.
21 H. Miyake, K. Chen, S. J. Lange and L. Que, Jr., *Inorg. Chem.*, 2001, **40**, 3534–3538.
22 S. J. Lange, H. Miyake and L. Que, Jr., *J. Am. Chem. Soc.*, 1999, **121**, 6330–6331.
23 M. P. Jensen, S. J. Lange, M. P. Mehn, E. L. Que and L. Que, Jr., *J. Am. Chem. Soc.*, 2003, **125**, 2113–2128.
24 J.-U. Rohde, J.-H. In, M. H. Lim, W. W. Brennessel, M. R. Bukowski, A. Stubna, E. Münck, W. Nam and L. Que, Jr., *Science*, 2003, **299**, 1037–1039.
25 K. Chen and L. Que, Jr., *Chem. Commun.*, 1999, 1375–1376.
26 I. W. C. E. Arends, K. U. Ingold and D. D. M. Wayner, *J. Am. Chem. Soc.*, 1995, **117**, 4710–4711.
27 D. W. Snelgrove, P. A. MacFaul, K. U. Ingold and D. D. M. Wayner, *Tetrahedron Lett.*, 1996, **37**, 823–826.
28 P. A. MacFaul, K. U. Ingold, D. D. M. Wayner and L. Que, Jr., *J. Am. Chem. Soc.*, 1997, **119**, 10594–10598.
29 P. A. MacFaul, I. W. C. E. Arends, K. U. Ingold and D. D. M. Wayner, *J. Chem. Soc., Perkin Trans. 2*, 1997, 135–146.
30 P. A. MacFaul, D. D. M. Wayner and K. U. Ingold, *Acc. Chem. Res.*, 1998, **31**, 159–162.
31 C. Walling, *Acc. Chem. Res.*, 1998, **31**, 155–157.
32 K. Neimann, R. Neumann, A. Rabion, R. M. Buchanan and R. H. Fish, *Inorg. Chem.*, 1999, **38**, 3575–3580.
33 A. Rabion, S. Chen, J. Wang, R. M. Buchanan, J.-L. Seris and R. H. Fish, *J. Am. Chem. Soc.*, 1995, **117**, 12356–12357.
34 C. Walling, *Acc. Chem. Res.*, 1975, **8**, 125–131.
35 M. J. Perkins, *Chem. Soc. Rev.*, 1996, **25**, 229–236.
36 K. U. Ingold and P. A. MacFaul, in *Biomimetic Oxidations Catalyzed by Transition Metal Complexes*, ed. B. Meunier, Imperial College Press, London, 2000, pp. 45–89.
37 (*a*) R. L. Donkers and M. S. Workentin, *Chem. Eur. J.*, 2001, **7**, 4012–4020; (*b*) M. S. Workentin and R. L. Donkers, *J. Am. Chem. Soc.*, 1998, **120**, 2664–2665.
38 (*a*) R. L. Donkers, F. Maran, D. D. M. Wayner and M. S. Workentin, *J. Am. Chem. Soc.*, 1999, **121**, 7239–7248; (*b*) M. S. Workentin, F. Maran and D. D. M. Wayner, *J. Am. Chem. Soc.*, 1995, **117**, 2120–2121.
39 R. L. Donkers, J. Tse and M. S. Workentin, *Chem. Commun.*, 1999, 135–136.
40 D. L. B. Stringle, R. N. Campbell and M. S. Workentin, *Chem. Commun.*, 2003, 1246–1247.
41 R. L. Donkers and M. S. Workentin, *J. Phys. Chem. B*, 1998, **102**, 4061–4063.
42 D. C. Magri, R. L. Donkers and M. S. Workentin, *J. Photochem. Photobiol. A: Chem.*, 2001, **138**, 29–34.
43 S. Antonello, M. Musumeci, D. D. M. Wayner and F. Maran, *J. Am. Chem. Soc.*, 1997, **119**, 9541–9549.
44 S. Antonello, F. Formaggio, A. Moretto, C. Toniolo and F. Maran, *J. Am. Chem. Soc.*, 2001, **123**, 9577–9584.
45 S. Antonello, F. Formaggio, A. Moretto, C. Toniolo and F. Maran, *J. Am. Chem. Soc.*, 2003, **125**, 2874–2875.
46 S. Antonello, M. Crisma, F. Formaggio, A. Moretto, F. Taddei, C. Toniolo and F. Maran, *J. Am. Chem. Soc.*, 2002, **124**, 11503–11513.
47 S. Antonello and F. Maran, *J. Am. Chem. Soc.*, 1999, **121**, 9668–9676.
48 S. Antonello and F. Maran, *J. Am. Chem. Soc.*, 1997, **119**, 12595–12600.
49 D. A. Casteel, *Nat. Prod. Rep.*, 1999, **16**, 55–73.
50 D. A. Casteel, *Nat. Prod. Rep.*, 1992, **9**, 289–312.
51 *Organic Peroxides*, ed. W. Ando, John Wiley & Sons Ltd, New York, 1992.
52 J.-M. Savéant, in *Advances in Physical Organic Chemistry*, ed. T. Tidwell, Academic Press, New York, 2000, vol. 35, pp. 117–192.

53 J.-M. Savéant, in *Advances in Electron Transfer Chemistry*, ed. P. S. Mariano, JAI Press Inc., Greenwich, CT, 1994, vol. 4, pp. 53–116.

54 J.-M. Savéant, *Acc. Chem. Res.*, 1993, **26**, 455–461.

55 K. Daasbjerg, S. U. Pedersen and H. Lund, in *General Aspects of the Chemistry of Radicals*, ed. Z. B. Alfassi, John Wiley & Sons, New York, 1999, pp. 385–427.

56 A. J. Bard and L. R. Faulkner, *Electrochemical Methods, Fundamentals and Applications*, 2nd edn., Wiley, New York, 2001.

57 The Butler–Volmer model of electrode kinetics implies the transfer coefficient is a constant over a potential range, which is contrary to the observed experimental results. See reference 56.

58 F. Maran, D. D. M. Wayner and M. S. Workentin, in *Advances in Physical Organic Chemistry*, ed. T. Tidwell and J. P. Richard, Academic Press, New York, 2001, vol. 36, pp. 85–166.

59 J. C. Imbeaux and J.-M. Savéant, *J. Electroanal. Chem.*, 1973, **44**, 169–187.

60 J.-M. Savéant and D. Tessier, *J. Electroanal. Chem.*, 1975, **61**, 251–263.

61 The background subtracted voltammograms are transformed to sigmoidal-shaped i–E curves by use of the convolution integral and the experimental current i. $I_{lim} = \pi^{-1/2} \int_0^t \frac{i(u)}{(t-u)^{1/2}} \, du$ The limiting current, I_{lim}, at the plateau of the sigmoidal-shaped i–E curves is under diffusion control and defined as $I_{lim} = nFAD^{1/2}C^*$ where n is the overall electron consumption, A is the electrode area, D is the diffusion coefficient, and C^* is the substrate concentration.

62 (*a*) For an irreversible electrode process I_{lim} and i are related to k^1_{het} by $\ln k^1_{het} = \ln \sqrt{D} - \ln\left(\frac{I_{lim} - I(t)}{i(t)}\right)$; (*b*) Derivatisation of the ln k^1_{het} allows the evaluation of the apparent transfer coefficient, a, uncorrected for the double layer. $\alpha = -\left(\frac{RT}{F}\right)\frac{\partial \ln k^1_{het}}{\partial E}$.

63 T. Lund and H. Lund, *Acta Chem. Scand., Ser. B*, 1987, **41**, 93–102.

64 N. T. Kjær and H. Lund, *Acta Chem. Scand.*, 1995, **49**, 848–852 . The rate constant for hydrogen atom abstraction by the *tert*-butoxyl radical was estimated to be 5×10^6 M^{-1} s^{-1}.

65 No *trans*-stilbene was observed as reported in the indirect reduction of some benzyl halides. See reference 63. Incidentally, dihydroanthracene and stilbene have the identical exact mass and similar GC retention times.

66 C. L. Perrin, J. Wang and M. Szwarc, *J. Am. Chem. Soc.*, 2000, **122**, 4569–4572.

67 J. A. Howard and J. Lusztyk, *Radical Reaction Rates in Liquids*, ed. H. Fischer, Landolt-Börnstein Group II, Springer-Verlag, Berlin, vol. 18, subvol. D1, 1997.

68 C. P. Andrieux, A. Le Gorande and J.-M. Savéant, *J. Am. Chem. Soc.*, 1992, **114**, 6892–6904.

69 H. Lund, K. Daasbjerg, T. Lund, D. Occhialini and S. U. Pedersen, *Acta Chem. Scand.*, 1997, **51**, 135–144.

70 C. P. Andrieux, J. M. Dumas-Bouchiat and J.-M. Savéant, *J. Electroanal. Chem.*, 1978, **87**, 39–53.

71 C. P. Andrieux, C. Blocman, J. M. Dumas-Bouchiat, F. M'Halla and J.-M. Savéant, *J. Electroanal. Chem.*, 1980, **113**, 19–40.

72 J.-M. Savéant and K. B. Su, *J. Electroanal. Chem.*, 1985, **196**, 1–22.

73 L. Nadjo, J.-M. Savéant and K. B. Su, *J. Electroanal. Chem.*, 1985, **196**, 23–34.

74 D. Occhialini, S. U. Pedersen and H. Lund, *Acta Chem. Scand.*, 1990, **44**, 715–719.

75 D. Occhialini, J. S. Kristensen, K. Daasbjerg and H. Lund, *Acta Chem. Scand.*, 1992, **46**, 474–481.

76 D. Occhialini, K. Daasbjerg and H. Lund, *Acta Chem. Scand.*, 1993, **47**, 1100–1106.

77 R. Fuhlendorff, D. Occhialini, S. U. Pedersen and H. Lund, *Acta Chem. Scand.*, 1989, **43**, 803–806.

78 S. U. Pedersen, T. Lund, K. Daasbjerg, M. Pop, I. Fussing and H. Lund, *Acta Chem. Scand.*, 1998, **52**, 657–671.

79 S. U. Pedersen and T. Lund, *Acta Chem. Scand.*, 1991, **45**, 397–402.

80 T. Lund, P. Christensen and R. Wilbrandt, *Org. Biomol. Chem.*, 2003, **1**, 1020–1025.

81 A. Cardinale, A. A. Isse and A. Gennaro, *Electrochem. Commun.*, 2002, **4**, 767–772.

82 K. Daasbjerg, *Acta Chem. Scand.*, 1993, **47**, 398–402.

83 R. A. Marcus and N. Sutin, *Biochim. Biophys. Acta*, 1985, **811**, 265–322.

84 D. D. M. Wayner, D. J. McPhee and D. Griller, *J. Am. Chem. Soc.*, 1988, **110**, 132–137.

85 P. Hapiot, V. V. Konovalov and J.-M. Savéant, *J. Am. Chem. Soc.*, 1995, **117**, 1428–1434.

86 S. U. Pedersen and K. Daasbjerg, *Acta Chem. Scand.*, 1989, **43**, 301–303.

87 K. Daasbjerg, S. U. Pedersen and H. Lund, *Acta Chem. Scand.*, 1991, **45**, 424–430.

88 D. D. M. Wayner and V. D. Parker, *Acc. Chem. Res.*, 1993, **26**, 287–294.

89 A comparison between di-*n*-propyl (37.1 kcal mol^{-1}), di-isopropyl (37.7 kcal mol^{-1}), and di-*tert*-butyl peroxide (37.4 kcal mol^{-1}) demonstrates that the BDE of acyclic peroxides is relatively independent of substituent. The BDFEs of BMPP and DMPP were estimated assuming the same BDE as DTBP and an entropy correction of $\Delta S = 28.5$ cal mol^{-1} K^{-1} (at 25 °C). The BDFEs for BMPP and DMPP are calculated to be 28.9 kcal mol^{-1}.

90 In the calculation of $E°_{BMPP}$, an average value for $E°_{RO'/RO^-}$ was used.

91 NIST Standard Reference Database; NIST Standard Reference Database and Properties Database and Estimation Program, U. S. Department of Commerce, Gaithersburg, MD, 2003.

92 S. W. Benson, *Thermochemical Kinetics*, 2nd edn., Wiley, New York, 1976.

93 The radius of BMPP and DMPP was determined from the density of the compound using the equation r (Å) $= 10^8[(3M/4\pi\rho N)^{1/3}]$.[53] Upon ET the charge is localised on the oxygen atom so an effective radius approach is used to better represent the size and molecular portion where the electron is accepted. The effective radius was determined using $r_{AB}^{eff} = [r_B(2r_{AB} - r_B)/r_{AB}]$, where r_{AB} is the radius of peroxide and r_B is the effective radius of the alkoxide anion. From the peroxide density radii, 4.44 and 4.71 Å for BMPP and DMPP, the effective radii were calculated as 2.83 and 2.87 Å, respectively. An average r_D of 3.80 Å was used for the donors. H. Kojima and A. J. Bard, *J. Am. Chem. Soc.*, 1975, **97**, 6317–6324.

94 $Z_{hom} = (r_D + r_{AB})^2 (8\pi RT/\mu)^{1/2}$ where r_D and r_{AB} are the radius of the donor and acceptor, and μ is the reduced mass. See reference 93.

95 J.-M. Savéant, *J. Phys. Chem. B*, 2002, **106**, 9387–9395.

96 $Z_{het} = (RT/2\pi M)^{1/2}$ where M is the molar mass.

97 K. Haghbeen and E. W. Tan, *J. Org. Chem.*, 1998, **63**, 4503–4505.

98 E. C. Horning, in *Synthesis of Azobenzene*, vol. 3, Wiley, London, 1955, p. 103.

99 P. G. Cookson, A. G. Davies and B. P. Roberts, *J. Chem. Soc., Chem. Commun.*, 1976, 1022–1023.

100 H. Masada and Y. Murotani, *Bull. Chem. Soc. Jpn.*, 1980, **53**, 1181–1182.

101 R. R. Hiatt and W. M. J. Strachan, *J. Org. Chem.*, 1963, **28**, 1893–1894.